Available online at www.sciencedirect.com

ScienceDirect

Energy Procedia 38 (2013) 430 – 435

Energy Procedia

SiliconPV: March 25-27, 2013, Hamelin, Germany

Ion-implanted PERC solar cells with Al_2O_3/SiN_x rear passivation

Thorsten Dullweber[a,]*, Rene Hesse[a], Vikram Bhosle[b], Chris Dubé[b]

[a]Insitute for Solar Energy Research Hamelin (ISFH), Am Ohrberg 1, 31860 Emmerthal, Germany
[b]Applied Materials, Varian Semiconductor Equipment, Gloucester, MA 01930-2297, USA

Abstract

Ion implantation is an attractive candidate for PERC solar cells due to the single-sided emitter phosphorus doping. The oxide, which is formed during the implant anneal, can be used as rear passivation of PERC cells. However, the SiO_2/SiN_x rear passivation is very sensitive to the rear surface roughness and surface preparation. Hence, in this paper we evaluate Al_2O_3/SiN_x rear passivation layers in combination with an oxide passivated ion-implanted emitter. We obtain emitter saturation current densities of 93 fA/cm^2, which is significantly lower compared to a typical $POCl_3$ diffused emitter with 140 fA/cm^2. Ion-implanted PERC cells with Al_2O_3/SiN_x rear passivation show conversion efficiencies up to 20.0% which is comparable to $POCl_3$-diffused PERC cells. The emitter dopant profile can be adjusted by the thermal budget of the anneal in order to optimize the process window between J_{sc} and *FF* losses. The IQE and reflectance of implanted and $POCl_3$-diffused PERC cells in the long wavelength regime are almost identical which demonstrates the successful implementation of the Al_2O_3/SiN_x rear passivation to PERC cells with ion-implanted emitters. Future work will focus on simplifying the process flow in order to obtain a lean industrially manufacturable PERC process, leveraging the single side doping via ion implantation.

© 2013 The Authors. Published by Elsevier Ltd. Open access under CC BY-NC-ND license.
Selection and/or peer-review under responsibility of the scientific committee of the SiliconPV 2013 conference

Keywords: Ion implantation; silicon solar cells; phosphorus emitter; Al_2O_3 rear passivation

1. Introduction

The single-sided doping of ion implantation as compared to the double-sided $POCl_3$ diffusion make ion implantation an interesting choice for passivated emitter and rear cell (PERC) processing where the rear side has to be non-phosphorus-doped. Efficiencies up to 19.7% were reported [1,2] for PERC solar cells

* Corresponding author. Tel.: +49-5151-999-638; fax: +49-5151-999-400
E-mail address: dullweber@isfh.de

1876-6102 © 2013 The Authors. Published by Elsevier Ltd. Open access under CC BY-NC-ND license.
Selection and/or peer-review under responsibility of the scientific committee of the SiliconPV 2013 conference
doi:10.1016/j.egypro.2013.07.300

with ion-implanted phosphorus emitter, a SiO_2/SiN_x rear passivation, and screen-printed metal contacts. With an advanced direct Ag printing method, 20.2% efficiency were achieved [1] thus demonstrating the potential of this approach. However, the SiO_2/SiN_x rear passivation requires rear surfaces with a small surface roughness in order to achieve good surface passivation properties [3,4,5]. In contrast, AlO_x/SiN_y rear passivation demonstrates excellent surface recombination velocities below 10 cm/s even for rough surfaces [5]. This increases the process window for industrial production and potentially enables higher conversion efficiencies. Accordingly, in this paper we evaluate industrial-type PERC solar cells applying an ion-implanted phosphorus emitter in combination with an ALD Al_2O_3/SiN_x rear passivation. We analyse the emitter saturation current density J_{0e} of the ion-implanted emitters and demonstrate PERC solar cells with screen-printed metal contacts showing conversion efficiencies of up to 20.0%.

2. Saturation current densities and dopant profiles of ion-implanted phosphorus emitters

Table 1: Sheet resistance R_{sheet} and emitter saturation current density J_{0e} of ion-implanted phosphorus emitters using two different annealing recipes, where recipe 1 has a higher thermal budget compared to recipe 2. As a reference, we include typical values of a $POCl_3$ diffused emitter.

Doping method	Anneal	R_{sheet} [Ω/sq.]	J_{0e} [fA/cm^2]
Ion implantation	Recipe 1	65	93
Ion implantation	Recipe 2	52	125
$POCl_3$ diffusion	n.a.	62	140

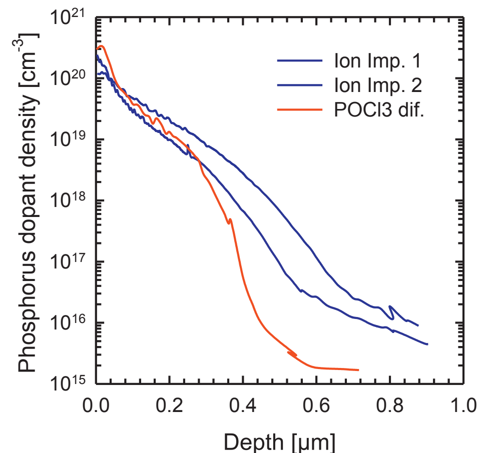

Fig. 1. Dopant profiles of the ion-implanted phosphorus emitters of table I measured by ECV profiling. As a reference, we include the dopant profile of the $POCl_3$-diffused emitter.

In order to analyze and optimize the J_{0e} of the ion-implanted phosphorus emitters, we use 200 Ω/sq. float zone (Fz) wafers. After cleaning and texturing, we implant phosphorus ions on both wafer surfaces using an implanter similar to the Applied Materials Solion tool [6]. We then anneal the implant crystal damage by a high temperature oxidation process, forming an approx. 25 nm thick SiO_2 layer on top of the phosphorus emitter. Afterwards, a SiN_x anti reflection coating is deposited on both wafer surfaces by

PECVD followed by a conventional furnace firing step as used for screen-printed metal contacts. Table I shows the resulting J_{0e} and emitter sheet resistance R_{sheet} values as measured by QSSPC. By using annealing recipe 1 we obtain a J_{0e} of 93 fA/cm^2 which is significantly lower compared to a conventional 62 Ω/sq. $POCl_3$-diffused emitter with a J_{0e} of 140 fA/cm^2. The 47 fA/cm^2 lower J_{0e} of the ion-implanted emitter *should allow* an approx. 4 mV higher open circuit voltage when applied to high efficiency PERC solar cells. The corresponding emitter dopant profiles measured by electrochemical voltage profiling (ECV) are shown in figure 1. In general, the dopant profiles of the ion-implanted emitters are quite similar to the $POCl_3$-diffused emitter. However, the phosphorus surface concentration of the implanted emitter is slightly lower which may explain the reduced J_{0e} values due to a reduced amount of inactive phosphorus atoms. When comparing the dopant profiles of the two implanted emitters in figure 1, the ion-implanted emitter 1 which applies the annealing recipe 1 in table 1 shows a slightly higher phosphorus surface concentration and a slightly shallower emitter due to the lower thermal budget of the annealing recipe 1 compared to annealing recipe 2.

3. PERC solar cells with ion-implanted phosphorus emitter and Al_2O_3/SiN_x rear passivation

3.1. PERC solar cell processing

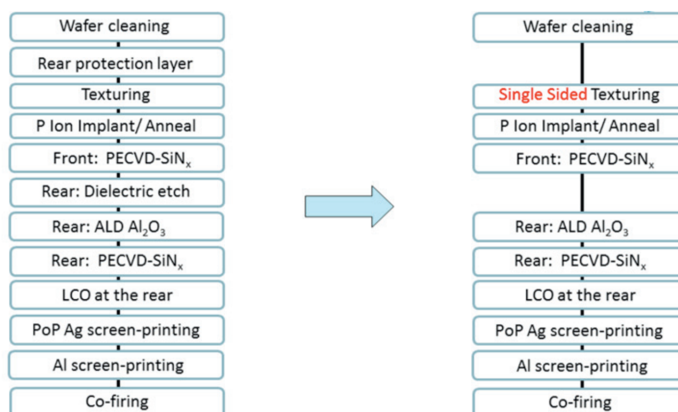

Fig. 2. The PERC cell process flow on the left side is used for the solar cells reported in this paper. The process flow on the right side is a future option for a lean industrial manufacturing process flow.

As a next step, we process PERC solar cells according to the process flow on the left side of figure 2. We use 156x156 mm^2 boron doped Cz wafers with a resistivity of 2 – 3 Ω*cm and a starting thickness of 190 µm. We obtain a single sided texturing of the front side using a rear protection layer which is removed later in the process flow. The phosphorus ions are implanted with the same implant parameters as used in table I and then annealed applying recipes similar to recipe 1 and 2 in table I. We deposit a SiN_x anti-reflective coating on the front side and then remove the dielectric on the wafer rear side with a diluted HF etch. Afterwards, we deposit the ALD Al_2O_3/SiN_x passivation stack on the wafer rear side followed by laser contact openings (LCO) to form line-shaped rear contacts. The metal contacts are deposited by print-on-print of Ag paste on the front side and full-area screen printing of Al paste on the rear side followed by drying and firing in conveyor belt furnaces. The resulting PERC solar cell is shown schematically in figure 3. As a reference, we also process PERC solar cells with $POCl_3$-diffused emitter

and ALD Al_2O_3/SiN_x rear passivation with a process flow very similar as described in Ref. 7. To assess the efficiency improvement due to the rear passivation, we process reference solar cells with full-area Al-BSF and implanted phosphorus emitter. Figure 2 shows on the right side one future option of a very lean process flow which is suitable for industrial manufacturing. Compared to the present process flow on the left side, we intend to remove the rear protection layer and apply a single sided alkaline texturing instead which then would allow to remove the dielectric etch later in the process flow as well. This work is, however, not yet part of this paper.

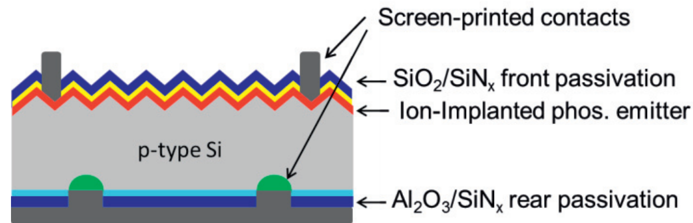

Fig. 3. Schematic drawing of the PERC solar cells with ion-implanted phosphorus emitter and Al2O3/SiNx rear passivation. The emitter is passivated with a SiO2/SiNx layer stack, the front and rear metal contacts are screen-printed with a local Al-BSF on top of the rear contacts.

3.2. PERC solar cell results

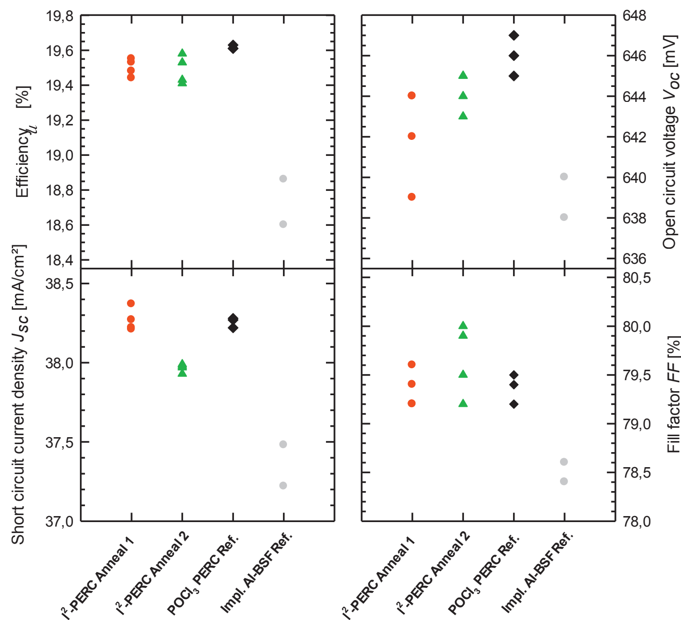

Fig. 4. IV parameters of ion-implanted (I2) PERC cells applying two different anneals and an ALD Al2O3/SiNx rear passivation. The anneal 2 has a higher thermal budget compared to anneal 1. For comparison, the IV parameters of POCl3-diffused PERC cells with ALD Al2O3/SiNx rear passivation as well as full-area Al-BSF cells with implanted emitter are shown. The IV parameters of the implanted PERC cells are quite similar to the POCl3-diffused PERC cells and show a good improvement in Voc and Jsc compared to the full-area Al.BSF cells

The resulting solar cell parameters of the ion-implanted (I^2) PERC cells with ALD Al_2O_3/SiN_x rear passivation are summarized figure 4. Anneal 2 has a higher thermal budget than anneal 1 which results in slightly lower short circuit current density J_{sc} values but higher fill factors FF and hence comparable efficiencies up to 19.6%. For comparison, the IV parameters of $POCl_3$-diffused PERC cells with ALD Al_2O_3/SiN_x rear passivation as well as full-area Al-BSF cells with implanted emitter are shown in figure 4 as well. The IV parameters of the implanted PERC cells are quite similar to the $POCl_3$-diffused PERC cells and show a good improvement in V_{oc} and J_{sc} compared to the full-area Al BSF cells. The best ion-implanted PERC solar cell demonstrates a conversion efficiency η of 20.0% as shown in table 2. For comparison, we include the values of our best $POCl_3$-diffused reference PERC cell. Within the limited statistics, we consider the implanted PERC and the $POCl_3$ PERC solar cell parameters as very similar. However, compared to the best full-area Al-BSF cell with implanted emitter in table II, the implanted PERC cell offers a 0.9% higher conversion efficiency.

Table 2. Solar cell parameters measured under standard testing conditions of the best PERC solar cell with ion-implanted emitter and ALD Al2O3/SiNx rear passivation. For comparison, the best POCl3-diffused PERC cell as well as the best solar cell with full-area Al-BSF are shown as well.

Solar cell type	Rear Passivation	η [%]	V_{oc} [mV]	J_{sc} [mA/cm^2]	FF [%]
Implanted PERC	Al_2O_3/SiN_x	20.0	659	38.7	78.3
POCl3 Reference PERC	Al_2O_3/SiN_x	19.7	659	38.7	77.3
Implanted Al-BSF	n.a.	19.1	643	37.4	79.6

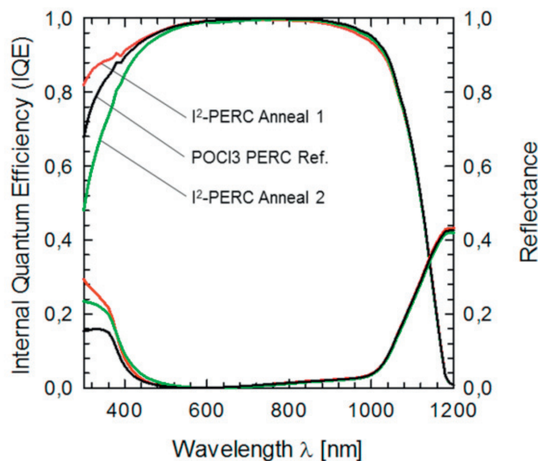

Fig. 5. IQE and reflectance measurements of the best cells of figure 4. The implanted PERC cell with anneal 1 shows the highest IQE in the blue wavelength regime probably due to the lowest emitter recombination as suggested by the J0e values of table I. As expected, the IQE and reflectance in the infrared wavelength regime are very similar which proofs the successful implementation of the Al2O3/SiNx rear passivation to PERC cells with ion-implanted emitters.

Figure 5 shows the IQE and reflectance measurements of the best PERC cells of figure 4. The implanted PERC cell with anneal 1 shows the highest IQE in the blue wavelength regime probably due to the lowest emitter recombination as suggested by the J_{0e} values of table I. However, all implanted PERC cells show a higher reflectance in the blue wavelength regime compared to the $POCl_3$ PERC cell due to

SiO_2/SiN_x layer stack which has a higher reflectance compared to a conventional SiN_x anti-reflective coating. As expected, the IQE and reflectance in the infrared wavelength regime are very similar for all PERC cells which proofs the successful implementation of the Al_2O_3/SiN_x rear passivation to PERC cells with ion-implanted emitters.

4. Conclusions

We have evaluated Al_2O_3/SiN_x rear passivation layers in combination with an oxide passivated ion-implanted emitter for industrial-type PERC solar cells. We obtain emitter saturation current densities of 93 fA/cm^2, which is significantly lower compared to a typical $POCl_3$ diffused emitter with 140 fA/cm^2. Ion-implanted PERC cells with Al_2O_3/SiN_x rear passivation show conversion efficiencies up to 20.0% which is comparable to $POCl_3$-diffused PERC cells. The emitter dopant profile can be adjusted by the thermal budget of the anneal in order to optimize the process window between J_{sc} and *FF* losses. The IQE and reflectance of implanted and $POCl_3$-diffused PERC cells in the long wavelength regime is almost identical which demonstrates the successful implementation of the Al_2O_3/SiN_x rear passivation to PERC cells with ion-implanted emitters. Further gain in conversion efficiency for ion implanted PERC cells are expected by incorporation of patterned ion implant (e.g. selective emitter) and advanced metallization. Future work will focus on adapting the process flow to industrial manufacturability, leveraging the single side patterned doping via ion implantation.

Acknowledgements

We thank our colleagues at Varian and ISFH for solar cell processing. Also, the continuous support of DEK, Heraeus, Ferro, and DuPont to advance our screen printing processes is gratefully acknowledged.

References

[1] Lai JH, Cooper IB, Chen X, Church K, Yang H, Rohatgi A. Large-area ~ 20% efficient silicon solar cells using fine line direct printing, *Proc. 38th IEEE PVSC Conf.*, Austin, USA (2012), p. 2192 - 5

[2] Mack S, Wolf A, Werner S, Dubé CE, Bhosle V, Biro D, Synergetic use of ion implant annealing processes for thermal oxide rear surface passivation, *Proc. 27th EUPVSEC Conf.*, Frankfurt, Germany (2012), p. 875 - 8

[3] Lai JH, Upadhyaya A, Ramanathan R, Das A, Tate K, Upadhyaya V et al.. Large area 19.6% efficient rear passivated silicon solar cells with local Al BSF and screen printed contacts, Proc. *37th IEEE PVSC Conf.*, Seattle, USA (2011), p. 1929 - 32

[4] Cornagliotti E, Uruena A, Horzel J, John J, Tous L, Hendrickx D et al.. How much rear polishing is required ? A study of the impact of rear side polishing in PERC solar cells, *Proc. 27th EUPVSEC Conf.*, Frankfurt, Germany (2012), p. 561-6

[5] Kranz C, Wyczanowski S, Dorn S, Weise K, Klein C, Bothe K, Dullweber T et al.. Impact of the rear surface roughness on industrial-type PERC solar cells, *Proc. 27th EUPVSEC Conf.*, Frankfurt, Germany (2012), p. 557 -60

[6] Dubé CE, Tsefrekas B, Buzby D, Tavares R, Zhang W, Gupta A et al.. High efficiency selective emitter cells using patterned ion implantation, *Energy Procedia* 2011; **8**: 706–711

[7] Dullweber T, Kranz C, Beier B, Veith B, Schmidt J, Roos BFP et al.. Inductively coupled plasma chemical vapour deposited AlOx/SiNy layer stacks for applications in high-efficiency industrial-type silicon solar cells, *Solar Energy Mat. Solar Cells* 2013; **112**: 196–201